Bulletin of Electrical Engineering and Informatics
Vol. 99, No. 1, Month 2099, pp. 1~1x
ISSN: 2302-9285, DOI: 10.11591/eei.v99i1.paperID

Silding-Mode Control Design of a Slotless Self-Bearing Motor

Vo Đuc Nhan [1], Nguyen Xuan Bien[2], Nguyen Quang Đich [1], Vo Thanh Ha[3*]
[1] Institute for Control Engineering and Automation- ICEA, Hanoi University of Science and Technology.
[2] Faculty of Mechanical Engineering, Thuy Loi University.
[3]Faculty of Electrical and Electrical Engineering, University of Transport and Communication
*Corresponding author E-mail: vothanhha.ktd@utc.edu.vn

Article Info

Article history:

Received month dd, yyyy
Revised month dd, yyyy
Accepted month dd, yyyy

Keywords:

Active Magnetic Bearing
Slotless Self-Bearing Motor
Self-Bearing Motor
Bearingless Motor
Sliding model Control, PID

ABSTRACT

Scientists have explored and are studying a slotless self-bearing motor, an electric motor with a magnetically integrated bearing function. As a single actuator, it can provide both levitation and rotation. This article will show a slotless self-bearing motor with a stator that does not have an iron core but six-phase coils. A permanent magnet and an enclosed iron yoke make up the rotor. To regulate the rotational speed and radial location of the rotor, magnetic forces created by the interaction between stator currents and the magnetic field of permanent interest are investigated. This research also includes a slotless-bearing motor mathematical model and control approach. This motor is investigated by combining an AC motor with a magnetic drive to achieve the essential design criterion and low cost. The magnetic force and moment characteristics are theoretically analyzed, and a control technique is proposed. Sliding-mode control (SMC) is a control method that is simple, effective and utilized to serve the control system for approaching the reference value, as stated in this study. It's also commonly used to manage the motor's position and speed. The findings were built and evaluated using Matlab/Simulink confirmed analytical results to prove the recommended control approach.

Corresponding Author:

Vo Thanh Ha
Faculty of Electrical and Electrical Engineering, University of Transport and Communication
HaNoi, VietNam
Email: vothanhha.ktd@utc.edu.vn

1. INTRODUCTION

The high speed and reliability requirements of many current industrial applications are well-known. Magnetic bearings are employed in these applications because they are contactless, lubricating, and need no maintenance. On the other hand, standard magnetic bearings take up a lot of space and maybe rather costly. As a result, it can only be used in restricted industrial settings. Numerous forms of study on slotless self-bearing motors have been conducted worldwide in the last ten years, with many compelling laboratory examples. Several papers have been published in. Prestigious scientific publications, including the. University of Kentucky's Laboratory of Mechatronics. For the slotless self-bearing motor, this lab provided deeper investigation and assessment. With multiple magnet poles, this motor may provide torque and lift.
Furthermore, when the magnet's thickness increases, the magnitude of the moment and the lifting force. increases. As a result, if the current and magnetic field of the attraction is just slightly different, this motor can

function reliably [1], [16-17]. They designed a self-bearing engine with a 152mm diameter, 25.4mm length, peak force of 213.6 N, and peak torque of 24Nm [2].

In recent years, the need to enhance, miniaturize, and boost mechanical and kinetic endurance has resulted in a significant development trend for compact engines [3-4],[12],[14] and [15]. Active magnetic bearings (ABM) seemed to fit that need nicely. There are several possibilities for employing ABM for tiny motors, but the high cost and big size restrict them compared to mechanical ball bearings. As a result, methods to replace magnetic bearings in small engines that fulfill size and cost requirements are required [5-6]. A 6-phase ABM has been proposed in response to this tendency. This construction has been complicated by the need toreduce the number of pole pairs and have a more compact design while yet fulfilling adequate magnetic force. Brushless DC motors have been significantly simplified in recent years. There are, motors on the market with a diameter of just 2mm. Combining a brushless dc motor with an active. magnetic drive is one suggestion. Based on such. characteristics. The typical structure of this suggested. engine type is shown in. Figure 1.1. The stator is wound without a steel core, and the magnet core is circular, the stator is encased in an iron sheath secured to the rotor. Thesuggested drive has a basic structure and meets the aims of simplicity and inexpensive cost.

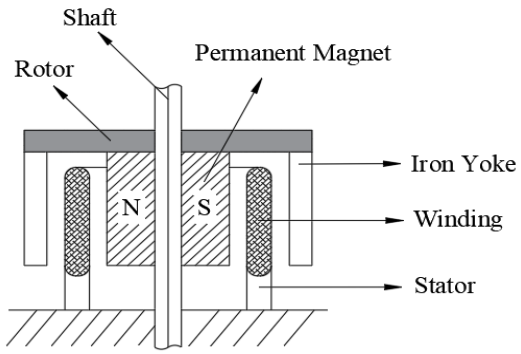

Figure 1. Structure of slotless self-bearing motor

The size of the self-bearing motor is reduced to the power density and performance of the self-bearing engine being improved. Simple open-loop and closed -loop torque control techniques have also been created. The results of the experiments show some of the engine's properties. On the other hand, these control systems are inadequate and superficial for current AC motor drives, resulting in poor dynamics and excessive displacement error. In most applications, the rotor should also be able to regulate precisely to cope with various operating needs and surroundings. Although the system's size may be reduced, the control becomes more complicated owing to the merged functions. As a result, improving system quality necessitates the creation of the controller. According to [7], [13], [18] the speed control is handled by a PI controller, while a PID takes the displacement position controller. The actual speed responds well and is close to the reference value. The controller boosts or reduces the current to assist lessen the deviation when there is a load torque. The phase stator currents take on a sinusoidal form following the speed shift.

Furthermore, the actual speed responds well and is near the reference value. When a load torque is present, the controller boosts or decreases the current to minimize deviation. With the change in speed, the phase stator currents take on a sinusoidal form. On the other hand, the actual rotor displacements are jumped from 0s to 0.1s. This indicates that the rotor has remained at the stator's center. As a consequence, when external forces are applied, the controller quickly removes the align deviation. However, the rotor's speed and. displacement overshoot during the transition point. As a result, a sliding-mode control system control has been suggested to increase control quality. Sliding-mode control is a control approach that uses a high-speed switching control law to force the system's trajectory onto the sliding surface. Because of its advantages, such as easy implementation finite-time convergence, strong dynamic. responsiveness, and resilience against parameter. fluctuations and disturbances, sliding-mode control is frequently employed in practical applications [8-9] and [19-21]. Furthermore, sliding-mode control's stability can. provide faultless tracking performance even when parameters or model uncertainties are present.

Based on the construction of sliding mode control and *dq* axis current regulation of a bearingless motor [10-11]. As a result, compared to the PID controller, this slotless self-bearing motor enhances position and speed control.

In addition, the suggested approach was simulated using Matlab/Simulink, and the simulation results demonstrated the system's good functionality. A mathematical model was described in the first section of this article. The second act is that of a control system designer. Finally, in the third and fourth parts, the findings were built and evaluated using Matlab/Simulink confirmed analytical data to prove the recommended control approach.

2. MATHEMATICAL MODEL

2.1. Introduction of the slotless self-bearing motor

The configuration of the SSBM is illustrated in Fig. 2. The rotor consists of a shaft, a cylindrical two-pole permanent magnet, a back yoke, and one part to fix them together. The air gap between the permanent magnet and iron yoke is invariable to ensure that the permanent magnet's unstable attractive force becomes zero. In addition, the iron yoke has a significant effect on reducing energy loss. The stator consists of a six-phase distributed winding without an iron core. This stator is inserted between the permanent magnet and the yoke of the rotor.

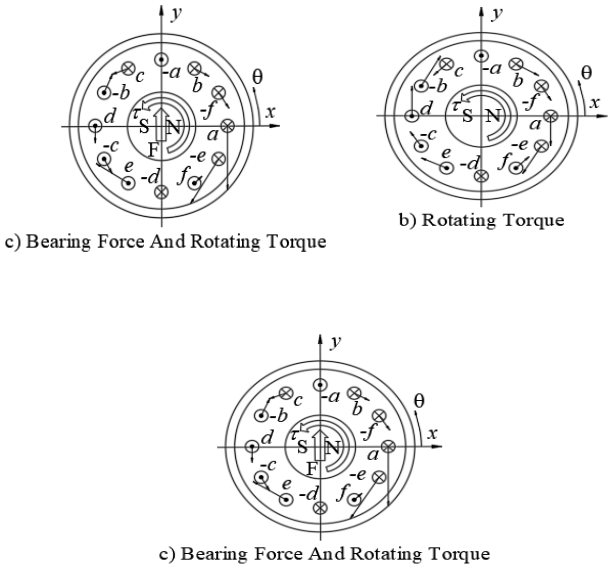

Figure 2. Generation of bearing force and rotating torque

The SSBM's working principle is seen in Fig.2. The number of spins in the stator winding is shown by a single circle, which shows the current direction. To simplify the mathematical model. A bearing force is created when currents are delivered to the stator coils, as illustrated in Fig. 2 (ab). On the other hand, the winds are fed to the stator coils, as indicated in Fig. 2 (b); the torque is generated as a response force on the rotor. Finally, as illustrated in Fig. 2, the torque and bearing pressure are created simultaneously by delivering both current types (c).

According to reference [7], the bearing force and torque have been calculated in detail. The stator currents are the summation of two components that generate bearing power and rotating torque. This makes the motor which can cause the bearing power and rotating torque simultaneously while the bearing force and torque can be controlled independently. The stator currents are supplied as follows:

$$\begin{cases} i_{a,d} = i_d \cos(\psi) + i_q \sin(\psi) \pm A_m \cos(\phi_m) \\ i_{b,e} = i_d \cos(\psi - 2\pi/3) + i_q \sin(\psi - 2\pi/3) \pm A_m \cos(\phi_m + \pi/3) \\ i_{c,f} = i_d \cos(\psi - 4\pi/3) + i_q \sin(\psi - 4\pi/3) \pm A_m \cos(\phi_m + 2\pi/3) \end{cases} \quad (1)$$

Where, i_d is the direct axis current; i_q is the quadrate axis current, ψ is the angular position of the rotor, A_m is the amplitude of the motor current, and ϕ_m is its phase.

We combine Eq. (1) with the stator winding properties to calculate the total force acting on the rotor and the generated torque.

The rotating torque and bearing forces in case of turns are obtained as follows:

$$\begin{cases} \tau = k_{nm} k_m A_m \sin(\phi_m - \psi + \theta_0 + \pi/4) \\ f_x = -k_{nb} k_b \ \ i_d \sin(2\theta_0) - i_q \cos(2\theta_0) \\ f_y = k_{nb} k_b \ \ i_d \cos(2\theta_0) + i_q \sin(2\theta_0) \end{cases} \quad (2)$$

With:

$$\begin{cases} k_m = -\left(3\sqrt{2} l_p + \dfrac{8(6-3\sqrt{2})}{\pi} l_t\right) rB \\ k_b = -\left(3 l_p + \dfrac{12}{\pi} l_t\right) B \\ k_{nm} = 1 + 2\cos\left(\dfrac{\pi}{3n}\right) + 2\cos\left(2\dfrac{\pi}{3n}\right) + \cdots + 2\cos\left(\dfrac{(n-1)}{2}\dfrac{\pi}{3n}\right) \\ k_{nb} = 1 + 2\cos\left(2\dfrac{\pi}{3n}\right) + 2\cos\left(4\dfrac{\pi}{3n}\right) + \cdots + 2\cos\left((n-1)\dfrac{\pi}{3n}\right) \end{cases} \quad (3)$$

Where τ is rotating torque, f_x and f_y are bearing forces, B is the amplitude of the magnetic flux density, l_p is the length of the parallel part of the winding, l_t is the length of the serial part of the winding, *n* is the total number of turns, and θ_0 is the angular position of the +a-phase winding. And *n* must be an odd number so that the wires may not overlap.

From Eq. (2), the mathematical model of the SSBM is completely constructed with force and torque equations. Next, we will go to design the control system for the SSBM.

3. DESIGNING THE CONTROL SYSTEM

3.1. Control structure

When the angular position of the rotor can be obtained, the stator current can be calculated by equation (1) and then, the force and torque are calculated by Eq.2. The θ_0 is the angular position of the +a-phase winding so if +a-phase coincides with x-axis then $\theta_0 = 0$. ϕ_m is the phase of the torque current and depends on control strategy. To conduct the clear control algorithm, we can assume that $\theta_0 = 0$ and $\phi_m = \psi + \dfrac{\pi}{4}$ or $\phi_m - \psi + \theta_0 + \dfrac{\pi}{4} = \dfrac{\pi}{2}$, then the equation (2) becomes:

$$\begin{cases} \tau = k_{nm} k_m A_m \\ F_x = k_{nb} k_b i_q \\ F_y = k_{nb} k_b i_d \end{cases} \quad (4)$$

It is easy to see that the rotating torque is produced by A_m and the bearing force is produced by i_d and i_q. Therefore, the rotating torque can be controlled by A_m and the bearing force can be controlled by i_d and, i_q. On the other hand, the two components force and torque are mathematically independent from each other, thus, the control structure is introduced as shown in Fig. 3. The sliding mode control is used for both the speed control and the displacement position control.

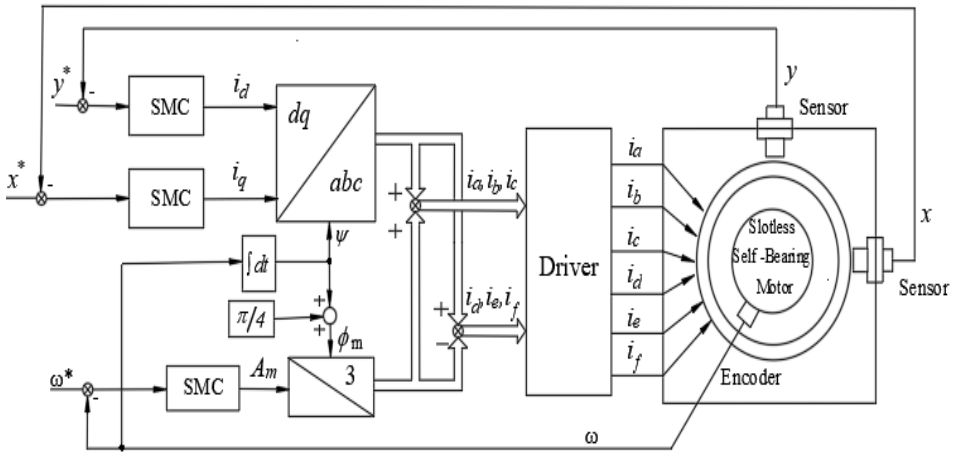

Figure 3. Control structure of the SSBM using sliding mode control

Sliding mode control is a well-known powerful control scheme which has been successfully and widely applied for both linear and nonlinear system. In this study, the linear sliding mode which using the linear sliding surface has been used to design the speed and position controller.

Setting: $K_T = k_{nm}k_m$ and $K_{fx} = K_{fy} = k_{nb}k_b$, the Eq. (4) becomes:

$$\begin{cases} \tau = K_T A_m \\ F_x = K_{fx} i_q \\ F_y = K_{fy} i_d \end{cases} \quad (5)$$

The dynamic equation of the rotor is:

$$\tau - T_l = J\frac{d\omega}{dt} \quad (6)$$

$$F - F_l = Ma \quad (7)$$

Where M is the weight of the rotor, a is the acceleration of the rotor, T_l is the load torque and F_l is the load force.

From Eq. (5) and Eq. (6) and Eq. (7), the transfer function models can be set up as shown in Fig. 5 and Fig. 6.

3.2. Desgning position controller

a. Designing position controller

Following Fig. 4 and Fig.5, assuming the effect of load torque and load force are the same as external disturbances, the mathematical model of the motor can be expressed as follows:

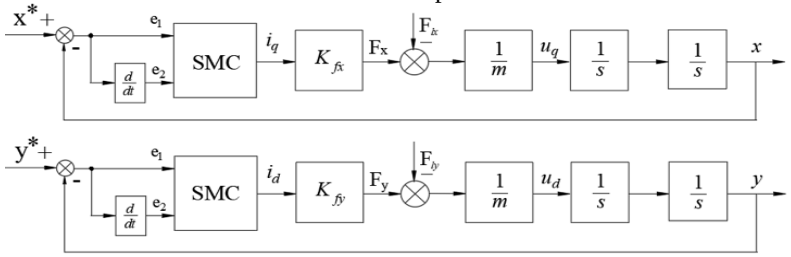

Figure 4. The position controller transfer function model

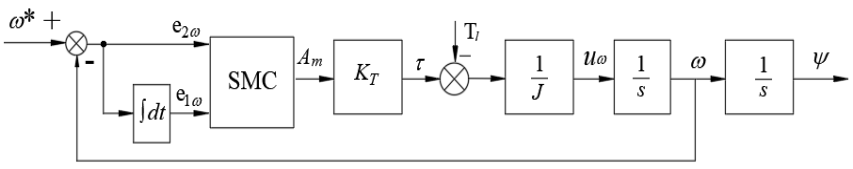

Figure 5. The speed controller transfer function mode

$$\begin{cases} \ddot{x} = \dfrac{K_{fx}}{m} i_q \\ \ddot{y} = \dfrac{K_{fy}}{m} i_d \\ \dot{\omega} = \dfrac{K_T}{J} A_m \end{cases} \tag{8}$$

Due to the parameters of two equations that generated bearing force being the same. Thus, design a sliding controller for both position controllers along the x-axis and y-axis. From the model in Fig. 8, setting:

$$K_f = \frac{K_{fx}}{m} = \frac{K_{fy}}{m}, u_d = K_f i_d, u_q = K_f i_q \tag{9}$$

At this time, we suppose that the controlled object is only a double integral $1/s^2$, using the sliding mode control for calculating parameter u_d , u_q and then come back to calculate current parameter i_d , i_q .

The controlled object $1/s^2$ is expressed as follows:

$$\frac{d\underline{x}}{dt} = \begin{pmatrix} x_2 \\ u \end{pmatrix} \text{ and } \underline{y} = x_1 \tag{10}$$

Where $\underline{x} = \begin{pmatrix} x_1 \\ x_2 \end{pmatrix}$ is the state vector, $\underline{y}$ is the output signal and $u = u_d = u_q$ is the control input.

Choosing the most commonly used sliding surface is the linear sliding surface which is:

$$s_1(e) = a_0 e_1 + e_2 \text{ and } \frac{de_1}{dt} = e_2 \tag{11}$$

Where e_1 is the position error, a_0 is a design parameter $a_0 > 0$ is chosen in order to the polynomial $P(s) = a_0 + s$ is Hurwitz polynomial which has the real parts of the roots smaller than zero [23], [24].

To guarantee the stability of the system, using the Lyapunov stability theory, in which the Lyapunov function has the form as:

$$V(s_1) = \frac{1}{2} s_1^2 \tag{12}$$

Then, the control design task become to make $\dot{V}(s_1) < 0$ in the neighborhood of the equilibrium. Thus, we have:

$$\frac{dV(s_1)}{dt} < 0 \Leftrightarrow s_1 \frac{ds_1}{dt} < 0 \Leftrightarrow \frac{ds_1}{dt} \text{sgn}(s_1(e)) < 0 \tag{13}$$

On the other hand:

$$\frac{ds_1}{dt} = a_0 \frac{de_1}{dt} + \frac{de_2}{dt} = a_0 \frac{de_1}{dt} - u \tag{14}$$

Thus, Eq. (13) becomes:

$$(a_0 \frac{de_1}{dt} - u) \text{sgn}(s_1(e)) < 0 \tag{15}$$

$$\Leftrightarrow a_0 \frac{de_1}{dt} - u = \begin{cases} < 0 & if \quad s_1(e) > 0 \\ > 0 & if \quad s_1(e) < 0 \end{cases} \tag{16}$$

$$\Leftrightarrow u = \begin{cases} > a_0 \dfrac{de_1}{dt} & if \quad s_1(e) > 0 \\ < a_0 \dfrac{de_1}{dt} & if \quad s_1(e) < 0 \end{cases} \tag{17}$$

Choosing the control input u as Eq. (18):

$$u = a_0 \frac{de_1}{dt} + k_0 \,\text{sgn}(s_1(\text{e})) \qquad \forall k_0 > 0 \tag{18}$$

From the Eq. (9) and Eq.(18), the current i_d , i_q are calculated as follows:

$$i_d = i_q = \frac{a_0 \frac{de_1}{dt} + k_0 \,\text{sgn}(s_1(\text{e}))}{K_f} \qquad \forall a_0, k_0 > 0 \tag{19}$$

Thus, Eq. (19) is the SMC used for the position controller. Next, the speed controller is also calculated correspondingly, but it has a difference from the reference signal.

b. Designing speed controller

Similar to the position controller, from the model in Fig. 9 setting:

$$K_{T\omega} = \frac{K_T}{J} \text{ and } u_\omega = K_{T\omega} A_m \tag{20}$$

The controlled object is still a double integral $1/s^2$, but the feedback signal is state variable, thus, the sliding surface is chosen:

$$\text{s}_\omega(\text{e}) = b_0 e_{1\omega} + e_{2\omega} = b_0 e_{1\omega} + \frac{de_{1\omega}}{dt} \tag{21}$$

Where $e_{2\omega}$ is the speed error, b_0 is a design parameter $b_0 > 0$ is the necessary condition.
Similar to the position controller, we have:

$$\text{s}_\omega \frac{ds_\omega}{dt} < 0 \Leftrightarrow \frac{ds_\omega}{dt} \text{sgn}(s_\omega(e)) < 0 \tag{22}$$

$$\Leftrightarrow \left(b_0 \frac{de_{1\omega}}{dt} + \frac{de_{2\omega}}{dt} \right) \text{sgn}(s_\omega(e)) < 0 \tag{23}$$

$$\Leftrightarrow (b_0 \frac{de_{1\omega}}{dt} - u_\omega) \,\text{sgn}(s_\omega(e)) < 0 \tag{24}$$

$$\Leftrightarrow b_0 \frac{de_{1\omega}}{dt} - u_\omega = \begin{cases} < 0 & if \quad s_\omega(e) > 0 \\ > 0 & if \quad s_\omega(e) < 0 \end{cases} \tag{25}$$

$$\Leftrightarrow u_\omega = \begin{cases} > b_0 \frac{de_{1\omega}}{dt} & if \quad s_\omega(e) > 0 \\ < b_0 \frac{de_{1\omega}}{dt} & if \quad s_\omega(e) < 0 \end{cases} \tag{26}$$

Choosing the control input u_ω as:

$$u = b_0 \frac{de_{1\omega}}{dt} + C.\text{sgn}(s_\omega(e)), \forall \text{C} > 0. \tag{27}$$

From the Eq. (20) and Eq.(27), the current A_m are calculated as follows:

$$A_m = \frac{b_0 \frac{de_{1\omega}}{dt} + C.\text{sgn}(s_\omega(e))}{K_{T\omega}} \qquad \forall b_0, C > 0 \tag{28}$$

Thus, Eq. (28) is the sling mode control which is used for the speed controller. From Eq. (19) and Eq. (28), the control system was designed. However, it is important to consider the well-known problem, namly, chattering, which is a not good oscillating phenomenon. For reducing the chattered phenomenon, $\text{sgn}(s)$ is replaced by a contiuous saturation function $sat(\text{s})$, which is defined as follows:

$$sat(\text{s}) = \begin{cases} \text{sgn}(s) & if \quad |s| > \varepsilon \\ \frac{s}{\varepsilon} & if \quad |s| \le \varepsilon \end{cases} \tag{29}$$

Where ε is the boundary layer thickness. However, although the sliding mode can be guaranteed outside the ε, it cannot be guaranteed inside the ε. This replacement can cause trajectory error.

To reduce both chattered phenomenon and trajectory error, a saturation-integral relay function (sat-Pi) is proposed which is defined as:

$$SatPi(s) = \begin{cases} \text{sgn}(s) & if \quad |s| > \varepsilon \\ \frac{s}{\varepsilon} + k_i \int_{t_0}^{t} s(t).dt & if \quad |s| \le \varepsilon \end{cases} \tag{30}$$

Where k_i is positive integral coefficient, t_0 is the time when the system state starts to reach ε .

4. SIMULATION AND RESULTS

We will develop a simulation model of the complete system using Matlab/Simulink in this part by modeling the motor in Section 2 and designing the control structures in Section 3.

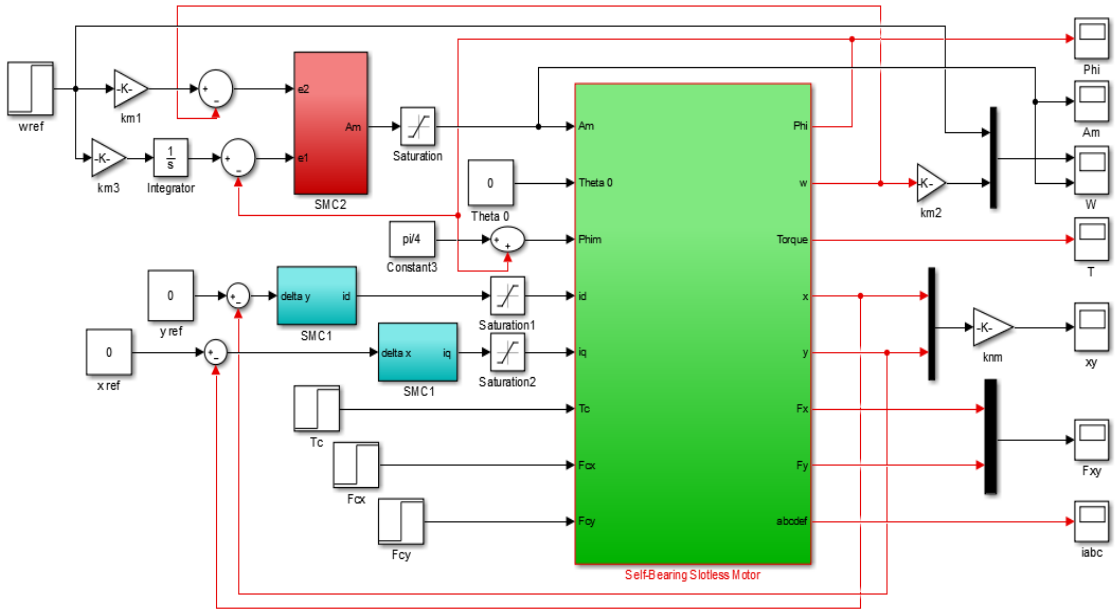

Figure 6. A simulation model of the complete system using Matlab/Simulink

Under sliding mode control, the recommended speed and position control solution attributes will be compared to PID control. The simulation results will be shown utilizing a Matlab/Simulink simulation in this research. Table 1 summarizes the simulation parameters.

Tabe. 1 Simulation Parameters

1. Motor parameters	Symbol	Value
Motor weight	m	0.4 Kg
Rotor radius	R	0.022 m
Stator radius	r	0.027 m
Flux maximum of the rotor	B	0.59 T
Length of the parallel part	lp	0.008 m
Length of the serial part	lt	0.006 m
The total number of turns	n	55
2. Controller parameters	**Symbol**	**Value**
Current-torque coefficients	km	-9.7×10^{-4}
Current-torque coefficients	knm	52.5
Current-force coefficients	kb	-0.0277
Current-force coefficients	knb	45.49
Position controller parameter	a0	150
Position controller parameter	k0	100
Speed controller parameter	b0	92
Speed controller parameter	C	56

The reference displacements x*,y* is set to 0 to maintain the rotor in the stator's center position. In addition, the simulation method is carried out according to the following scenarios to demonstrate the capabilities of independent control between speed and radial position:

+ *Position control*: The beginning locations are x0 = -0.3mm and y0 =0.3mm, with a speed of 0. Actual displacements and currents are tested for their reactions shown in Fig. 7.

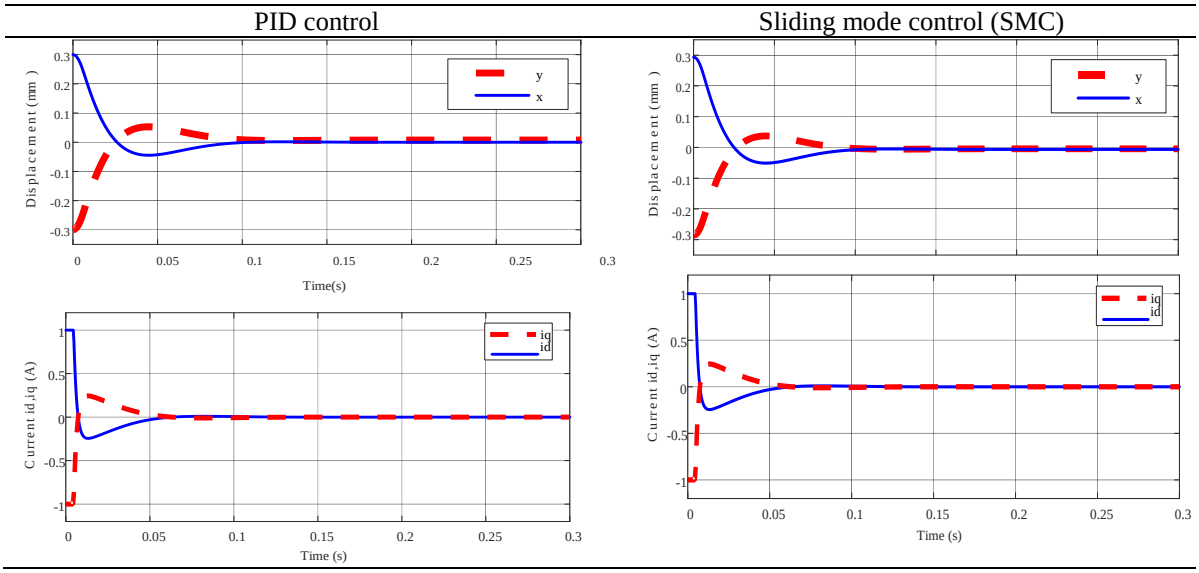

Figure 7 Displacement and stator current responses

The simulation results of the position controller for both controls showed that depicts the rotor's radial displacements in x, y, and current directions x=0.3 mm and y=-0.3mm were the initial displacement errors. The dis-placements then jumped to zero after roughly 0.04 s when the position controller began working. External im-pulse forces (Flx=1N, Fly=0.3N) operating on the rotor in the *x, y* directions at the duration of 0.1s were present when the position controller operated stably. The rotor's position remained almost unaltered during this period. It demonstrates that the position controllers can withstand disruptions.

+ *Speed control*: the reference speed is *rpm* without. At the time of t=1s with at the reference speed is +500 rpm, then at the time of 2s the speed is reduced to +200rpm next at the time of 3s, the rotation direction is reversed to -200 rpm and at the time of 4s the reference speed is -500 rpm. The responses of the speed and currents are considered. The simulation results using the speed controller are displayed in Fig.8. Both control methods showed that the actual speed responds well and is close to the reference value. Quick set-up time 0.1s at acceleration and reverse, when the motor is operating at speeds of +500 rpm to -500 rpm. However, in the high-speed range from +3000 rpm to -3000prm, the speed response of the SMC controller gives a faster response time than the PID controller at acceleration and reverse. In addition, the phase stator currents have a sinusoidal form and are restricted by the speed change to a value of -1A to 1A.

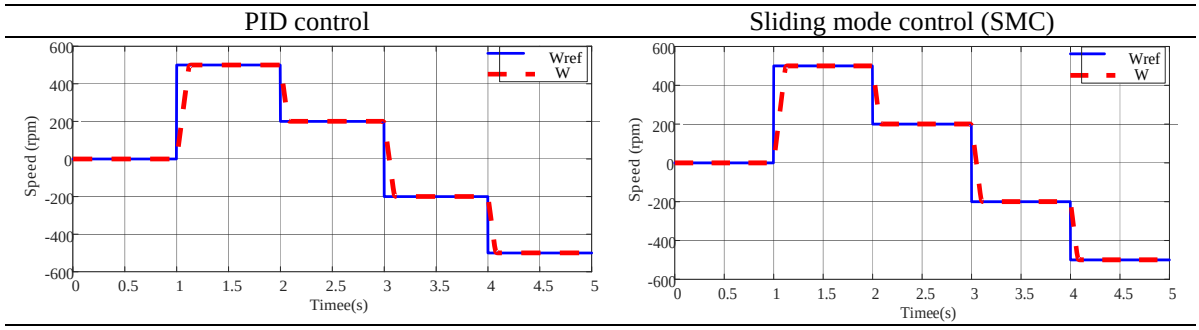

Speed responses

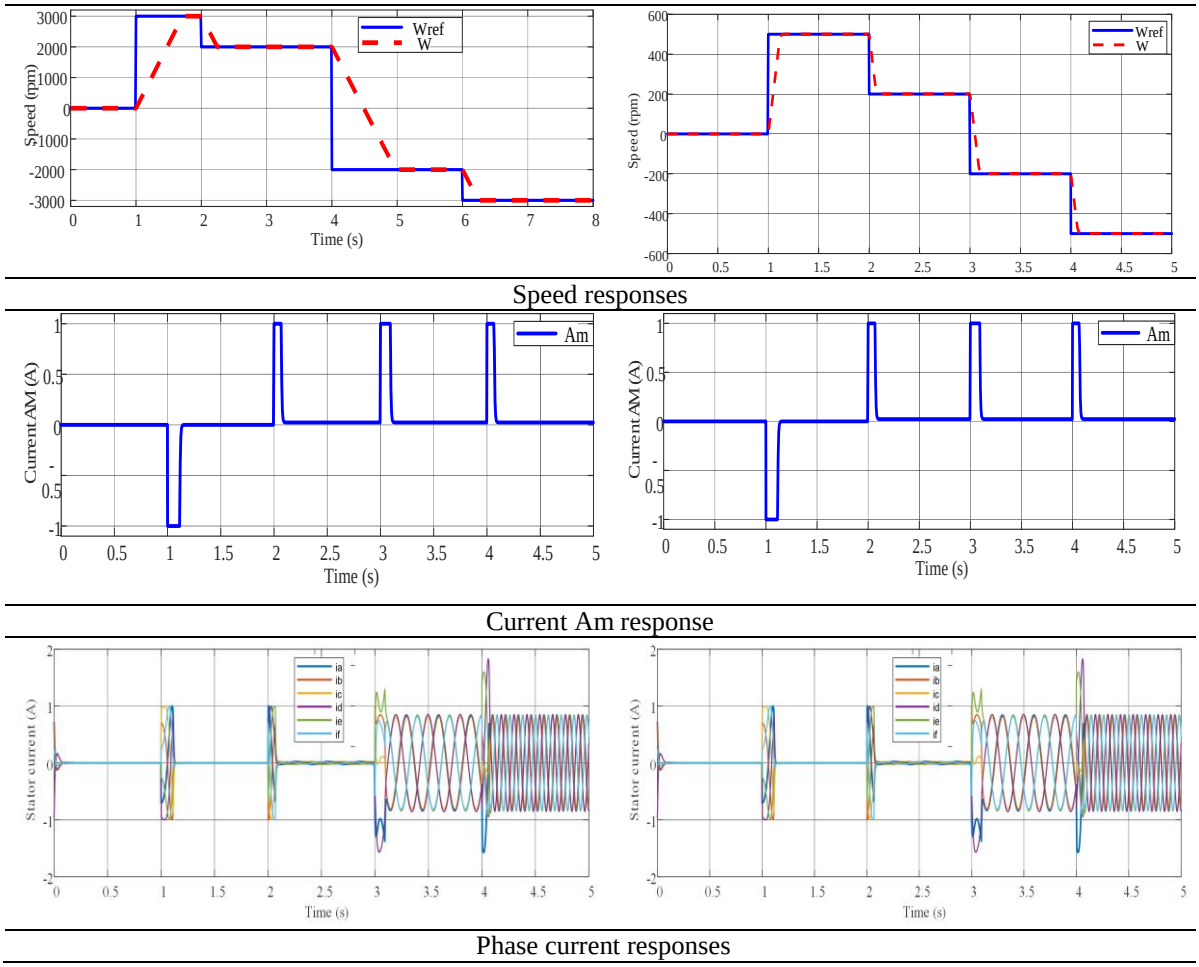

Figure 8. Speed and current Am, phase current responses

ACKNOWLEDGEMENTS

The authors would like to thanks Institute for Control Engineering and Automation of Ha Noi University of Science and Technology for their assistance.

4. CONCLUSION

The slotless self-bearing motors can manufacture specialized engines that require high performance, large power density, and simple structure. This paper analyzed the slotless self-bearing motor's operating principle and calculation method as torque and bearing forces. In addition, the analysis and design of sliding mode control for rotating speed and radial position are also presented in more detail. The simulation results for sliding mode control compared with PID control showed that the rotating speed and rotor position are controllable and good speed response than more at high speed. Furthermore, slotless self-bearing motors could operate stably with the proposed control method.

REFERENCES

[1] Y. Okada et al, JSME, Publiccation on New Technology Series, No. 1, *Magnetic Bearing – Fundamental Design and Applications (in Japanese)*, Yokendo Ltd. Tokyo .1995.
[2] S. Ueno et al, *Development of the Miniture AMB with 6 Concentated Wound Poles*, Proceedings of 9th International Symposium on Magnetic Bearings, CD-ROM.2004.
[3] Technology Overview of Allied Motion Technologies Inc.
[4] Salazar, A. O., Chiba, A., and Fukao, T., *A Review of Developments in Bearingless Motors, Proc. 7th Int. Symp. Magn. Bearings*, ETH, Zurich, Aug. pp. 335–339.2000.

[5] L. Li et al, *A Simple a Miniaturized Magnetic Bearing for Cost-Sensitive Applications*, Proceedings of 9th International Symposium on Magnetic Bearings, pp. 561-565.2002.
[6] Jeffrey Hillyard, *Magnetic Bearings (Joint Advanced Student School),* Department of Mechanical Engineering - Technical University of Munich.2006.
[7] Nguyen HP, Nguyen XB, Bui TT, Ueno S, Nguyen QD, *Analysis and Control of Slotless Self-Bearing Motor*, *Actuators*. 2019; 8(3):57.
[8] V. Utkin, J. Guldner, and J. X. Shi, *Sliding Mode Control in Electromechanical Systems.* London, U.K.: Taylor and Francis, 1999.
[9] V. Utkin, *Sliding Modes in Control and Optimization*. Berlin, Germany: Springer-Verlag, 1992, ser. Communications and Control Engineering Series.
[10] S. Kobayashi and M. Ooshima, *A Radial Position Control Method of Bearingless Motor Based on d-q Axis Current Control,* IEEE Trans. Ind. Appl. 2013, 49, 1827–1835.
[11] M. Ooshima, S. Kobayashi, and M. N. Uddin, *Magnetic levitation tests of a bearingless motor based on d-q axis current control*, in Proceedings of the 2012 IEEE Industry Applications Society Annual Meeting, Las Vegas, NV, USA, 7–11 October 2012.
[12] Y. Okada, K. Dejima and T. Ohishi; *Analysis and comparison of PM synchronous motor and induction motor type magnetic bearing*. IEEE Trans. Industry Applications, vol. 32.1995 pp. 1047-1053.
[13] T. Baumgartner, R. Burkart and J.W. Kolar, *Analysis and Design of an Ultra-High-Speed Slotless Self-Bearing Permanent-Magnet Motor,* IECON 2012 - 38th Annual Conference on IEEE Industrial Electronics Society.
[14] T.I. Baumgartner, A. Looser, C. Zwyssig, and J.W. Kolar, Novel High-Speed, Lorentz-Type, Slotless SelfBearing Motor, 2010 IEEE Energy Conversion Congress and Exposition.
[15] Hooi-Mei Chin, L. Scott Stephens, *Closed Loop Performance of a Slotless Lorentz Self Bearing Motor*, Journal of Computing and Information Science in Engineering Journal of Dynamic Systems, Measurement, and Control Journal of Electrochemical Energy Conversion and Storage, GT2003-38750, pp. 583-591; 9 pages, February 4, 2009.
[16] Budi Azhari, Pudji Irasari, Puji Widianto, *Design and simulation of 5kW BLDC motor with half-buried permanent magnets using an existing stator body*, Vol. 12, No. 4, December 2021, pp. 2030~2043 ISSN: 2088-8694, DOI: 10.11591/ijpeds.v12.i4.pp2030-2043, International Journal of Power Electronics and Drive Systems (IJPEDS).
[17] Ridwan Gunawan, Feri Yusivar, Budiyanto Yan, *The Self Excited Induction Generator with Observation Magnetizing Characteristic in the Air Gap*, Vol. 5, No. 3, February 2015, pp. 355~365, International Journal of Power Electronics and Drive Systems (IJPEDS).
[18] N. N. Baharudin, S. M. Ayob, *Brushless DC Motor Speed Control Using Single Input Fuzzy PI Controller*, Vol. 9, No. 4, December 2018, pp. 1952~1966, International Journal of Power Electronics and Drive Systems (IJPEDS).
[19] Abdellatif Hinda, Mounir Khiat, Zinelaabidine Boudjema, *Advanced control scheme of a unifiedpower flow controller using sliding mode control*, Vol. 11, No. 2, June 2020, pp. 625~633, International Journal of Power Electronics and Drive Systems (IJPEDS).
[20] Jung-Woo Cheon, Seung-Bok Choi, Hyun-Jeong Song and Joon-Ho Ham, *Position Control of an AC Servo Motor Using Sliding Mode Controller with Disturbance Estimator*, International Journal of Precision Engineering and Manufacturing Vol. 5, No.4, October 2004.
[21] Navaneethan, Jovitha Jerome, *Speed control of Permanent Magnet Synchronous Motor using Power Law based Sliding Mode Controller*, Volume 10, 2015, Weas Transaction on Systems and Control.

BIOGRAPHIES OF AUTHORS

Quang Dich Nguyen received the B.S. degree in electrical engineering from Hanoi University of Technology, Hanoi, Vietnam, in 1997, the M.S. degree in electrical engineering from Dresden University of Technology, Dresden, Germany, in 2003, and the Ph.D. degree from Ritsumeikan University, Kusatsu, Japan, in 2010. Since 2000, he has been with Hanoi University of Science and Technology, Vietnam, where he is currently an Associate Professor and the Executive Dean of the Institute for Control Engineering and Automation. His research interests include magnetic bearings, self-bearing motors, and sensor-less motor control. (Based on document published on 20 September 2021).

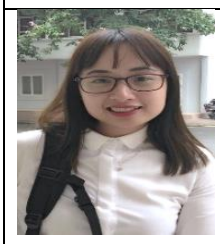

Vo Thanh Ha received the B.S degree in Control, and Automation Engineering from Thai Nguyen University of Technology, Vietnam, in 2002, the Master's degree from Hanoi University of Science and Technology, Vietnam, in 2004. She received a Ph.D. degree from Hanoi University of Science and Technology, Viet Nam, in 2020, both in Control and Automation Engineering. She has worked at the University of Transport and Communications as a lecturer since 2005. Her current areas of research are electrical drive and power electronics.